The Incorporation of Quantum Effects in Enzyme Kinetics Modeling

DONALD G. TRUHLAR,* JIALI GAO,* CRISTOBAL ALHAMBRA, MIREIA GARCIA-VILOCA, JOSÉ CORCHADO, MARIA LUZ SÁNCHEZ, AND JORDI VILLÀ

Department of Chemistry and Supercomputer Institute, University of Minnesota, 207 Pleasant Street SE, Minneapolis, Minnesota 55455-0431

Received July 31, 2001

ABSTRACT

We present an overview of new procedures for including quantum mechanical effects in enzyme kinetics. Quantum effects are included in three ways: (1) The electronic structure of the atoms in the catalytic center is treated quantum mechanically in order to calculate a realistic potential energy surface for the bond rearrangement process. (2) The discrete nature of quantum mechanical vibrational energies is incorporated in the treatment of nuclear motion for computing the potential of mean force. (3) Multidimensional tunneling contributions are included. These procedures are illustrated by applications to proton abstractions catalyzed by enolase and methylamine dehydrogenase and hydride-transfer reactions by alcohol dehydrogenase and xylose isomerase.

1. Introduction

The calculation of reaction rates for enzyme-catalyzed processes is a central goal of computational biological chemistry. There are several key points in our treatment:

(1) The free energies of reactants and transition states are critical determinants of reaction rates. Variational transition-state theory (VTST) and potential of mean force (PMF) calculations provide useful tools for identifying transition states,[1−3] and an important goal of the work summarized here is to extend VTST to enzymatic reactions by employing PMF calculations to identify transition-state ensembles.

(2) Quantum effects are very important in modeling chemical reaction rates, especially the inclusion of tunneling and zero-point vibrational energy throughout the reaction.[4,5] Importantly, we can obtain good accuracy with multidimensional semiclassical tunneling approximations.[6−8]

(3) By using semiclassical methods, calculations of reaction rates can be carried out by using a manageably localized portion of the potential energy surface (PES).[4,6] Most enzyme reactions occur on the ground-electronic-state PES, and the Born−Oppenheimer approximation is generally valid; here we restrict ourselves to this case. It is well known that the regions of the PES in the vicinities of reactant and product geometries can be reasonably well described by molecular mechanics (MM). Major effort has gone into developing and refining MM potential energy functions capable of describing proteins and protein−coenzyme−substrate interactions. The regions of the PES between reactants and products that is necessary to describe the chemical step has partially broken and/or partially made bonds, and they require a quantum mechanical (QM) treatment of their electronic structure in order to model their PES. A critical advance summarized here is the combination of QM methods for the subsystem involving partial bonds with MM methods for the rest of the enzyme−coenzyme−substrate system; such hybrid methods are usually called combined QM/MM methods.[2,9]

Thus, quantum mechanical effects must be included in three key aspects of the modeling of enzyme reac-

* To whom correspondence should be addressed. E-mail: truhlar@umn.edu and gao@chem.umn.edu.

Donald G. Truhlar was born in Chicago in 1944. In 1965 he received a B.A. from St. Mary's College of Minnesota, and in 1970 he received a Ph.D. from Caltech, where his adviser was Aron Kuppermann. In 1969, he joined the Chemistry faculty of the University of Minnesota, where he was promoted to Professor in 1976 and where he is currently Institute of Technology Distinguished Professor. He married his wife Jane in 1965, and they have two children, Sara and Stephanie.

Jiali Gao was born in 1962. He received a B.S. degree in chemistry from Beijing University in 1983 and a Ph.D. from Purdue University. He was a postdoctoral associate at Harvard with Martin Karplus and held a faculty position at SUNY—Buffalo until 1999. He is currently Professor of Chemistry at the University of Minnesota. He enjoys Minnesota's weather and its wilderness.

Cristóbal Alhambra was born in Barcelona, Spain, in 1967. He received a bachelor degree in 1990 and completed a Ph.D. in chemistry from the University of Barcelona in 1996, on computational studies of the molecular recognition of DNA by small molecules with Pr. Modesto Orozco and Pr. Javier Luque. He joined the group of Jiali Gao at SUNY—Buffalo and later at the University of Minnesota, working on development of combined quantum mechanical/classical mechanical techniques and their application to enzyme reactivity, as a postdoctoral research associate until 2001. He is presently a research scientist at AstraZeneca, and his interests are in the study of the molecular recognition and reactivity of enzymes using computational methodologies.

Mireia Garcia-Viloca was born in Barcelona, Spain, in 1972. She received a B.A. degree in chemistry from the Universitat Autònoma de Barcelona under the supervision of José Ma. Lluch and Àngels González-Lafont. She came to the United States through a Fulbright/Regional Government of Catalonia Visiting Scholar Program to join Jiali Gao's group at the University of Minnesota, where she is presently a Postdoctoral Associate.

José C. Corchado was born in Badajoz, Spain, in 1969. He received a doctorate in chemistry from the University of Extremadura (Spain) in 1996 and completed a Fulbright postdoctoral fellowship in chemistry at the University of Minnesota in 1998. He is currently a postdoctoral researcher at the University of Extremadura. His research program includes reactivity in the gaseous and condensed phases in collaboration with the University of Minnesota.

Maria Luz Sanchez Mendoza was born in Caceres, Spain, in 1967. She has been working for the University of Extremadura in Spain since 1992. She got a degree in chemistry in 1990 and a doctorate in 1997 from this university and has also worked for the University of Pisa in Italy and the University of Minnesota as a postdoctoral researcher. Her main research fields are the theoretical study of molecular interactions and the development of models for chemical and biological processes in solution.

Jordi Villà received a B.Sc. and Ph.D., both in chemistry, at the Universitat Autònoma de Barcelona, in 1993 and 1998, respectively. He was a postdoctoral fellow with Donald G. Truhlar at the University of Minnesota and with Arieh Warshel at the University of Southern California, holding an EMBO fellowship. He is currently a Ramón y Cajal researcher at the Universitat Pompeu Fabra in Barcelona, Spain, and he is also committed to teaching. His scientific interests are in the field of enzyme reactivity and macromolecular interactions, and he is currently involved in the modeling of signal transduction processes. He is the father of two children.

10.1021/ar0100226 CCC: $22.00
Published on Web 03/03/2002

tions: calculation of the PES, computation of vibrational energy along the reaction path, and estimation of tunneling contributions.

Enzyme reactions have aspects that require special considerations not involved in modeling simpler reactions in the gas phase. Proteins are flexible solutes with well-defined secondary, tertiary, and quaternary structure that is essential to their activity. Incorporating the three-dimensional shape of the enzyme as well as its flexibility and computing the free energy profile along the reaction path provide challenges to the molecular modeling of enzyme behavior that will be considered in this Account.

2. The Potential Energy Surface

Early work in QM/MM methods demonstrated its power[2,10−13] and exposed the need for special attention to the boundary region where QM methods for the subsystem are joined to MM methods for its surroundings. Two subsequent formalisms that have proved convenient and successful for treating the boundary region are strictly localized bond orbitals[14] and generalized hybrid orbitals[15] (GHOs). Both methods eliminate the need for the troublesome "link" atoms of earlier work.[11,12] We use the GHO approach, which appears to be more robust.

The Born−Oppenheimer energy of the system is the sum of the QM energy of the QM subsystem, the MM energy of the MM subsystem, and their interaction.[2] The MM subsystem is bonded to the QM one at N_B boundary atoms, each of which is chosen to be an sp^3 carbon of the MM subsystem. The QM part is treated by a molecular orbital calculation employing a linear combination of atomic orbitals (AOs); the AOs consist of a minimum basis set of N_Q orbitals from the fully QM subsystem plus $4N_B$ hybrid AOs. Only one hybrid orbital from each boundary atom is optimized in the self-consistent-field process, which therefore involves $N_Q + N_B$ AOs. The boundary atom is treated as a QM atom in the QM energy calculation but as an MM atom in connection with the MM subsystem. Matrix elements between AOs of the QM subsystems are calculated in a standard semiempirical way.[16] The matrix elements involving orbitals on the boundary atom were parametrized by calculations on simple alkanes.[15]

We note that the semiempirical model is typically qualitatively reasonable[16] but quantitatively inaccurate. This is checked by preliminary calculations on the enzyme reaction or on model systems. If quantitative inadequacies need to be addressed, the semiempirical model is corrected either by adding a few-body semiempirical valence bond (SEVB) term or by adjusting the parameters of the semiempirical QM matrix elements for the specific reaction of interest. This adjustment can be carried out either by adjusting parameters to experiment or by adjusting them to higher level calculations. The adjusted parameters are called specific reaction parameters[17] (SRPs).

In all applications presented in this Account, the molecular mechanics parameters used for enzymes are taken from the CHARMM22 force field,[18] and those for water are taken from the TIP3P[19] model.

3. Dynamics

The rate constant for a unimolecular reaction at temperature T is approximated as[1,20]

$$k(T) = \gamma(T)\frac{\tilde{k}T}{h}\exp[-\Delta G^{CVT}(T)/N_A\tilde{k}T] \qquad (1)$$

where $\gamma(T)$ is the transmission coefficient, $\tilde{k}$ is Boltzmann's constant, h is Planck's constant, $\Delta G^{CVT}(T)$ is the standard-state molar free energy of activation calculated by canonical VTST (usually abbreviated as canonical variational theory, or CVT), and N_A is Avogadro's number. As discussed below, the factor $\tilde{k}T/h$ relates the equilibrium one-way flux through the transition state to the equilibrium constant for formation of the transition state; $\gamma(T)$ as well as $\Delta G^{CVT}(T)$ depends on the solute environment. Since experimental data are often expressed as

$$k(T) = \frac{\tilde{k}T}{h}\exp[-\Delta G_{act}/N_A\tilde{k}T] \qquad (2)$$

where ΔG_{act} is the phenomenological standard-state molar free energy of activation, we have

$$\Delta G_{act} = \Delta G^{CVT}(T) - N_A\tilde{k}T\ln\gamma(T) \qquad (3)$$

Thus, there are two critical quantities to be calculated: $\Delta G^{CVT}(T)$ and $\gamma(T)$.

For gas-phase reactions, the transition state has traditionally been defined as a species missing one degree of freedom, called s, the reaction coordinate.[1] To make further progress, it is essential to translate this into mathematical terms; the transition state becomes a hypersurface in phase space or configuration space dividing reactants from products, and the reaction coordinate is normal to this surface.[21] We specify the hypersurface by two parameters, z_* and Ω, where z_* denotes its location along some progress variable z on a path from reactants to products, and Ω denotes the shape and orientation of the hypersurface. The hypersurface is called a generalized transition state (GT). The fundamental assumption of transition-state theory is that the reaction rate equals the one-way equilibrium flux through this hypersurface. If classical mechanics were valid, and if the hypersurface is a hyperplane in rectilinear coordinates, this assumption gives[22]

$$k(T) = \frac{\tilde{k}T}{h}\exp\{-[G^{GT}(T,z_*,\Omega) - G^R(T)]/N_A\tilde{k}T\} \qquad (4)$$

where $G^R(T)$ is the free energy of reactants and $G^{GT}(T,z,\Omega)$ is an integral over the phase space of the hypersurface; this integral is identical in form to the expression for the free energy of a system constrained to be in the GT. The exponential function in eq 4 is the equilibrium constant for forming the transition state. It can be shown that, provided the reactants are in local equilibrium (a reasonable assumption), eq 4 provides an upper bound to the

accurate classical rate constant.[21,22] If one would completely optimize the hypersurface not just in coordinate space but in phase space, one would get the exact local equilibrium rate constant. Furthermore, if one does not optimize the transition-state hypersurface, the calculated one-way flux is larger than the net flux due to trajectories that recross the hypersurface.[1] These are rigorous results in a classical world, but the real world is quantum mechanical. From this point on, the theory becomes less rigorous but more relevant to real molecules such as enzymes and their substrates.

When one relaxes the assumption that the dividing hypersurface is a hyperplane, the identification of the one-way flux with a free energy, as in eq 4, becomes approximate, but for chemically reasonable dividing surfaces it is usually assumed to be a good approximation, and we make this approximation. The best result is obtained by minimizing eq 4 with respect to the location z and shape and orientation Ω of the hypersurface, which is equivalent to maximizing $G^{GT}(T,z,\Omega)$. Then,

$$\Delta G^{CVT}(T) = \max_{z,\Omega} G^{GT}(T,z,\Omega) - G^{R}(T) \qquad (5)$$

For gas-phase reactions we have obtained very good results[1,7,8] by proceeding as follows: (1) Let z be the curvilinear distance (arc length) along the isoinertial minimum energy path (MEP). (2) Rather than optimizing Ω, choose the dividing hypersurface to be normal to the MEP on the MEP (so that the missing coordinate s is taken locally as the progress coordinate z) and extend it off the MEP in a reasonable way, without including a correction for non-hyperplanarity. (3) Quantize the free energies in the harmonic approximation to calculate ΔG^{CVT}. (4) Include quantum mechanical effects on the reaction coordinate, which is the coordinate excluded from $G^{GT}(T,z,\Omega)$, by using a transmission coefficient based on an optimized multidimensional tunneling[23] (OMT) approximation. The OMT approximation includes zero-point effects in the effective potential for tunneling[24] and optimizes the tunneling path by a practical version of a least imaginary action[25] principle.

A critical element in the multidimensional tunneling calculations is that the tunneling path is not on the MEP but rather on its concave side, due to the negative internal centrifugal effect of a quantum system (due to its negative kinetic energy).[26] This is sometimes called corner-cutting tunneling. In many cases the optimized result for calculating tunneling reduces to using the centrifugal-dominant small-curvature tunneling approximation,[27] in which the tunneling path is implicitly displaced from the MEP in the direction of the reaction path curvature by approximately the amplitude of a zero-point vibrational amplitude transverse to the MEP. For large curvature of the reaction path, the displacement can be greater.[4,6,23,25]

Note that, in principle, $\gamma(T)$ can include two kinds of effect, and one could write

$$\gamma(T) = \kappa(T)\Gamma(T) \qquad (6)$$

where $\kappa(T)$ is greater than unity and accounts for the increased flux through the transition state due to tunneling (as discussed above), and $\Gamma(T)$ is less than unity and accounts for the dynamic recrossing events that are omitted by the one-way flux approximation in transition-state theory.[1] We have generally achieved excellent results for gas-phase reactions with $\Gamma(T) = 1$.[1,4,7,8]

The next level of complexity, beyond the gas phase, is reactions in liquid solutions. The assumption of equilibrium internal state distributions for reactants and transition states is usually quite reasonable in both the gaseous and liquid states, but occasionally it is suspect, which can cause the phenomenological rate to differ from the local equilibrium one,[28] or even not to exist.[29] We continue, however, to assume local equilibrium along the reaction coordinate z. A second issue of equilibration, which should not be confused with local equilibrium of the solute or substrate internal degrees of freedom, is equilibration of the solvent or protein polarization with respect to changes in the coordinates of the solute or substrate. For reactions of small organic molecules in liquids, this issue is the question of equilibrium[3] or nonequilibrium[30−32] solvation. Any approach in which the solvent participates in the reaction coordinate includes nonequilibrium solvation to some extent. If instead, the solvent is equilibrated to the solute (equilibrium solvation), the solute can be described as moving under the statistically averaged force of the solvent, leading to a solute PMF.[33] The clear distinction between solute and solvent coordinates for reactions of small molecules in liquids allows one to include quantum mechanical vibrations in the solute analogously to the way they are included in the gas phase.[2,34] For enzyme reactions, there is no clear-cut solute−solvent border unless we treat the whole enzyme, coenzyme (if any), and substrate as a solute, which is not the most practical approach. Furthermore, we do not want to assume equilibrium polarization. Therefore, we proceed differently. First, we single out a chemically motivated reaction coordinate z, and we compute a fully coupled classical mechanical PMF with respect to this single z. Then, to incorporate quantum mechanical effects, we define primary and secondary subsystems[35−37] to include average quantum mechanical vibrational free energy and tunneling contributions; the division into subsystems is a generalization of an embedded cluster model used previously for processes at gas−crystal interfaces.[38] The border between primary and secondary subsystems in the dynamics step can be the same as the QM/MM border for calculating the PES, but it need not be.

For enzyme reactions, we proceed in three stages, the first of which has two steps. In stage 1, we pre-define the shape and orientation of the dividing surfaces such that they correspond to constant z, and we set

$$z = r_B - r_M \qquad (7)$$

where r_B is the instantaneous bond length of the breaking bond, and r_M is that of the making bond. Further, we let z^R denote the value of z that corresponds to the reactant (the Michaelis complex). Step one of stage 1 does not use the separation into primary and secondary subsystems,

but later stages do. In step one of stage 1,[35−37] we use classical mechanical umbrella sampling[39] to calculate the PMF on z. For rectilinear z, the PMF is equal to $G^{GT}(T,z,\Omega)$ within a constant that can be computed from the free energy of reactants. In step 2, instantaneous generalized normal-mode analysis[5] is carried out for a subsystem to include quantum vibrational energies for many configurations sampled during the umbrella sampling simulation. We carry out instantaneous normal-mode analysis for the atoms that are used in the definition of z and the atoms that are most strongly coupled to these atoms; this typically includes the substrate molecule and residues or coenzymes in the active site. These atoms constitute the primary subsystem, and the rest of the enzyme−solvent system is called the secondary subsystem or the bath. For the generalized normal-mode frequencies so obtained, we estimate the difference, called $\Delta W_{vib}(T,z)$, between the primary subsystem's quantum mechanical and classical mechanical vibrational free energy, and this is added to the classical PMF along z. This yields a quasiclassical (QC) free energy of activation by maximizing $G^{GT}(T,z,\Omega) + \Delta W_{vib}(T,z)$, and by setting the transmission coefficient equal to unity, we obtain a QC rate constant since the reaction coordinate is still classical at the GT.[37] (Note that the reaction coordinate is excluded from the instantaneous generalized normal modes of the GT by a projection operator.[5])

In stages 2 and 3, we build on the quasiclassical value of $G^{CVT}(T,z)$, but we no longer assume that the transmission coefficient is unity. Stage 2 differs from stage 3 in the way that the protein−solvent potential field is included in the primary zone dynamics calculations.[37] In either stage, the transmission coefficient γ is an ensemble average over reaction paths of the primary system corresponding to transition-state configurations obtained during the umbrella sampling calculation of stage 1. Each individual γ_i consists of two factors, $\gamma_i = \Gamma_i\kappa_i$, with one factor Γ_i being an approximation to the dynamic recrossing transmission coefficient[20,21,40,41] and the other factor κ_i accounting for the increase in the rate due to quantum mechanical tunneling contributions. The latter factor is defined by extending the definitions of a consistent CVT transmission coefficient that were used earlier in the gas phase,[1] in embedded clusters in solids,[38] and in liquid solution.[3] The ensemble averages of γ_i, κ_i, and Γ_i are denoted by γ, $\langle\kappa\rangle$, and$\langle\Gamma\rangle$, respectively.

In stage 2, the effective potential for the calculation of the transmission coefficient γ_i is computed in the static (frozen) potential field of configuration i. The transmission coefficient γ obtained in stage 2 is called the ensemble-averaged static secondary zone (EA-SSZ) transmission coefficient.[37] Even in stage 2, the calculation includes a realistic estimate of the entropic contributions of all the low-frequency modes, which are included in the PMF and hence in eq 1. Furthermore, the high-frequency modes of the primary system are quantized, as they should be.

In stage 3, the effective potential used to evaluate the transmission coefficient includes the change in free energy

Scheme 1. Stepwise Mechanism for the Enolase Reaction

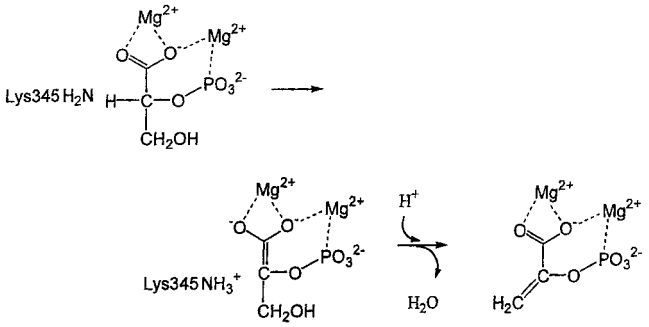

of the secondary system along the primary system reaction coordinate in an average way, by assuming that the secondary zone is equilibrated to the primary zone. This stage of the calculation is performed by equilibrating the secondary zone to the primary one at points along the reaction path by using free energy perturbation[42] theory. The transmission coefficient in stage 3 is averaged over reaction paths, each with the solvent equilibrated along the path; consequently, it is called the ensemble-averaged equilibrium secondary zone (EA-ESZ) approximation.[37] One could imagine an even more sophisticated treatment in which the secondary zone motion is included but without assuming it is equilibrated, but so far we have not done this for enzymes. Such a treatment would be required to allow the secondary zone atoms or the polarization of distant parts of the enzyme or solvent to participate even more fully in the reaction coordinate. It is important to note that, because the reaction coordinate used for the transmission coefficient depends on the secondary zone configuration, the secondary zone does participate in the reaction coordinate, and the ensemble-averaged transmission coefficients do not assume equilibration of the secondary zone to the solute. Thus, the calculation involves nonequilibrium polarization of the secondary zone. Although stage 3 is much more expensive than stage 2, it is not clear, a priori, whether the ensemble average of the frozen or equilibrated secondary zone is a better approximation.

For the applications presented below, stochastic boundary molecular dynamics[43] and umbrella sampling at 300 K or a specified temperature were performed for all residues with any atom within a 24-Å sphere centered on the substrate molecule.

4. Applications

4.1. Enolase. Enolase catalyzes the proton-transfer reaction in the conversion of 2-phospho-D-glycerate (2-PGA) to phosphoenolpyruvate. Primary and secondary kinetic isotope effects (KIEs) provided strong evidence for a stepwise mechanism (Scheme 1), involving the initial formation of a carbanion intermediate by abstraction from the carbon acid at the C-2 position, which is followed by the removal of the β-hydroxyl group.[44,45] We[35] obtained a QC free energy of activation of 14.5 kcal/mol. The corresponding experimental value is 15.0 kcal/mol. A significant finding is that the effect of treating the vibrations by

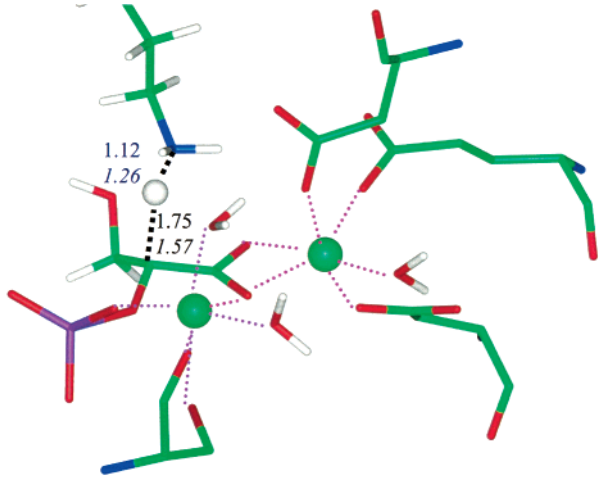

FIGURE 1. Active site of the proton-transfer reaction catalyzed by enolase. The substrate is on the left, and the Lys345 side chain is on the right. The breaking and making bond distances (in angstroms) are shown for the variational transition states for H^+ abstraction (top) and D^+ abstraction (bottom).

Table 1. Primary Kinetic Isotope Effect for Deuteron Transfer in Enolase at 300 K

		$k_H(T)/k_D(T)$			$k_H(T)/k_D(T)$
semiclassical	TST	4.7	classical	TST	1.4
	CVT	3.7		CVT	1.3
	CVT/SCT	3.5	experiment		3.3

quantum mechanics is large, reducing the QC free energy of activation by 2.1 kcal/mol from the CM value of 16.8 kcal/mol. Tunneling further lowers ΔG_{act} by 0.3 kcal/mol ($\langle\kappa\rangle = 1.7$).

The computed KIEs for deuteron transfer[35] are listed in Table 1. We find excellent agreement with experiment when quantum effects are included, but not when the calculations are classical. The reason is illustrated in Figure 1, which compares the CVT geometries for proton and deuteron transfer. For deuteron transfer, the CVT transition state has $r_B = 1.57$ Å and $r_M = 1.26$ Å, which are within 0.01 Å of values at the saddle point. However, because the zero-point energy associated with the forming N−H bond increases more rapidly than the potential energy decreases, the variational transition state for proton transfer deviates significantly from the saddle point, resulting in CVT geometries of $r_B = 1.75$ Å and $r_M = 1.12$ Å.

4.2. Alcohol Dehydrogenase. The work of Klinman and co-workers on liver alcohol dehydrogenase (LADH) provides experimental evidence for hydrogen tunneling.[46,47] We carried out simulations[35,36] to determine whether KIEs can be accurately predicted for such enzymatic reactions and to determine to what extent tunneling contributes to this reaction.

LADH catalyzes the reversible conversion of an alcohol to an aldehyde (Figure 2). We obtained a QC free energy of activation of 14.7 kcal/mol for the oxidation of benzyl alcoholate anion. For comparison, the experimental phenomenological value is 15.6 kcal/mol. The good absolute agreement with experiment confirms the reasonableness of the potential, which involves parameters calibrated[36] using ab initio calculations on model compounds, X-ray structure data for Zn interactions, and experimental data on the free energy profile in the enzyme. The QC free energy of activation is 1.8 kcal/mol lower than the CM result. A similar quantization effect of 1.8 kcal/mol was calculated by Hammes-Schiffer and co-workers by using an empirical potential energy function and mixed quantum/classical molecular dynamics,[48] in encouraging agreement.

The stage 2 transmission coefficient γ was averaged over 18 configurations of the transition state. Although the frozen bath approximation in the stage 2 calculation is reasonable for the short time scale of the barrier crossing, we further incorporated the dynamic contributions of the surrounding protein−solvent bath in our stage 3 algorithm, which yielded $\gamma = 4.1$.[37] This exceeds unity because of tunneling ($\langle\Gamma\rangle = 0.98$, so $\gamma \cong \langle\kappa\rangle$), and it is essential to include tunneling effects to obtain accurate KIEs (Table 2). The total effect of quantizing nuclear motion on ΔG_{act} is 2.6 kcal/mol. A preliminary study[49] of this oxidation reaction by a path-integral method with an empirical potential energy has also been carried out.

Our study[36,37] provides insight into the critical portion of the tunneling process that is responsible for exhaltation of the secondary H/T Swain−Schaad exponent. As the C−H bond begins to break during the hydride-transfer reaction, there is significantly more tunneling for the case of secondary H than for the case of secondary T; about half of this increase is due to participation of secondary hydrogen in the reaction path, and about half is due to a greater probability for corner-cutting tunneling.

4.3. Methylamine Dehydrogenase. Methylamine dehydrogenase (MADH) is a quinoprotein that converts primary amines to aldehyde and ammonia (Scheme 2), and large primary KIEs of 5−55 have been observed for the proton-transfer step.[50,51]

We found[52] that the net effect of the inclusion of the quantum mechanical nature of vibrational free energy and the effect of the average Γ_i (the dynamic recrossing transmission coefficient) in stage 2 reduces the CM free energy of activation from 20.3 kcal/mol to a value of 17.1 kcal/mol. Tunneling effects further lower the free energy of activation by 2.5 kcal/mol, resulting in a theoretical value of 14.6 kcal/mol at 298 K, in good accord with the experimental value of 14.2 kcal/mol at 303 K. This overall lowering of the activation barrier by 5.7 kcal/mol illustrates the need to incorporate quantum mechanical vibrational free energies and tunneling contributions into enzyme kinetics.

The tunneling effects ($\Delta\Delta G_{act} = 2.5$ kcal/mol) in the proton-transfer reaction in MADH are much larger than those for the reactions in enolase and LADH, where tunneling reduces the free energy of activation by 0.3 and 0.8 kcal/mol, respectively. In MADH, tunneling is an important factor in the absolute reaction rate, increasing the rate constant by a factor of $\langle\kappa\rangle = 84$ (see Table 3, and note that the ratio of the CVT/SCT and QC rate constants is $\{\langle\kappa(T)\Gamma(T)\rangle\}/\{\langle\Gamma(T)\rangle\}$, where the average value of $\Gamma(T)$

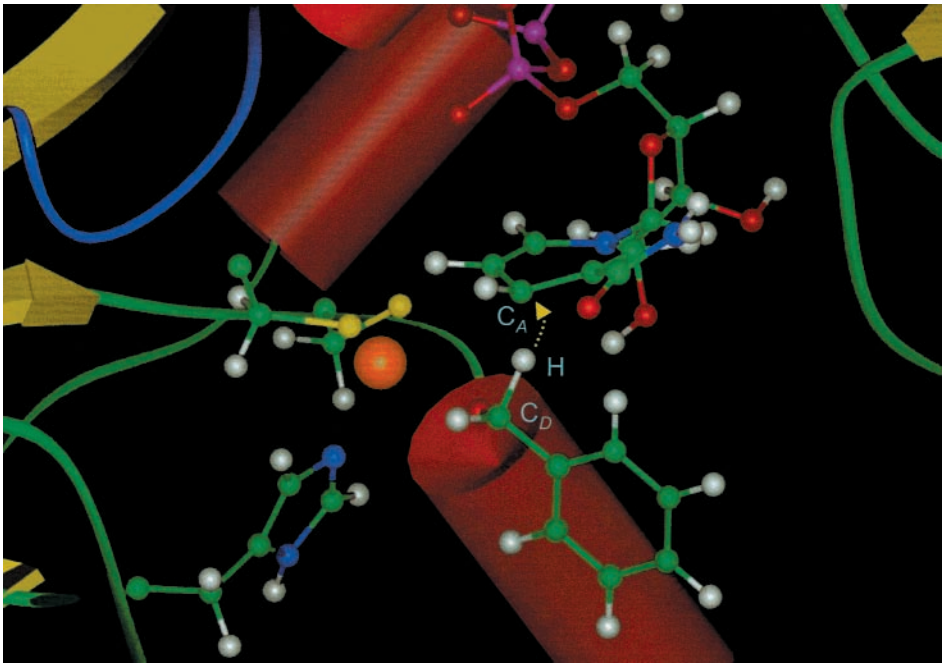

FIGURE 2. Benzyl alcoholate substrate in the active site of LADH in the act of transferring a hydride ion from the donor carbon atom to the acceptor carbon on NAD^+. The alcoholate anion is in the first coordination shell of a zinc cation (shown in orange), which also has three protein residues in its first ligation shell. The rest of the protein is in the background.

Table 2. Primary and Secondary Kinetic Isotope Effects for Oxidation of Benzyl Alcoholate Anion Catalyzed by NAD^+ and LADH at 300 K

		CVT/SSZ			CVT/ESZ		
		CVT	ZCT	μOMT	ZCT	μOMT	expt[a]
primary[b]	k_H^H/k_T^H	6.7	6.6	6.9	5.2	7.5	7.1 (7.3−7.8)
	k_D^D/k_T^D	1.8	1.8	1.8	1.8	1.7	1.9 (1.8−1.9)
secondary[b]	k_H^H/k_H^T	1.09	1.18	1.26	1.21	1.36	1.33 (1.31−1.32)
	k_D^D/k_D^T	1.02	1.04	1.05	1.12	1.08	1.07 (1.03−1.05)

[a] References 46 and 47. Wild-type value is shown first, followed by values for mutants in parentheses. [b] Notation: $k^{\text{secondary}}_{\text{primary}}$.

is 0.76 for the CH_3 case). Our calculations indicate that about 1% of the reaction occurs by overbarrier processes, with the rest due to tunneling.

A KIE of 18.3 was obtained for the all-protium versus the trideuterium reaction in MADH, as compared with the experimental value[50] of 17.2. The good agreement of theory and experiment for this KIE provides evidence that our tunneling calculations are semiquantatively accurate and hence provides the most striking evidence yet for the contribution of tunneling processes to enzymatic reactions at physiological temperatures. Conventional TST without tunneling yields a considerably smaller KIE value of 5.9 due to zero-point energy loss in a C−H/D stretch as the reaction progresses toward the transition state.

4.4. Xylose Isomerase. Xylose isomerase (XyI) catalyzes the interconversion of glucose and fructose (xylose and xylulose under physiological conditions) and is one of the most widely used enzymes in industry. It has also begun to receive theoretical attention.[53,54] An important aspect of the active site of XyI is the involvement of two metal ion cofactors (Mg^{2+} ions) bridged by Glu216. X-ray crystal

Scheme 2. Key Reaction Steps in Methylamine Dehydrogenase

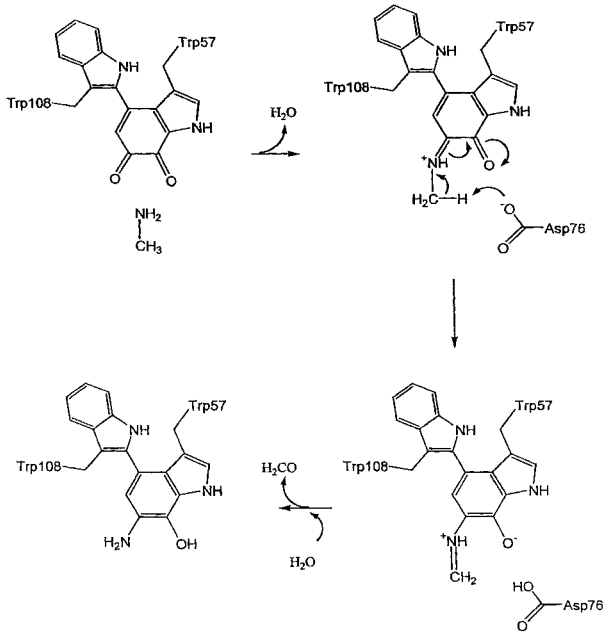

structures showed that the movements of the Mg^{2+} ions are intimately involved in the enzyme-catalyzed reaction.[55]

We[56] used two models to determine the PMF for the hydride-transfer reaction whose mechanism[57] is depicted in Scheme 3; these models contain the same number of atoms in the simulation system, but they differ in the partition between the QM and MM parts. Model 1 treats the electronic structure of all 19 atoms of the substrate xylose (with its O-2 deprotonated) as QM, whereas in model 2, the Mg ions and the side chains of all their ligands are also included in the QM region, giving rise to a total of 79 QM atoms. The rate constants were calculated

Scheme 3. Proposed Key Mechanistic Steps for the Isomerization of Xylose to Xylulose in Xylose Isomerase (Scheme Shows Residues Discussed in the Text)

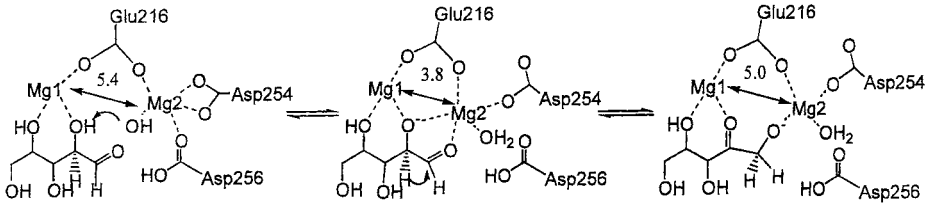

Table 3. Computed Classical Mechanical, Quasiclassical, and CVT/SCT Rate Constants for the Proton- and Deuterium-Transfer Reaction in Methylamine Dehydrogenase, and Primary Kinetic Isotope Effect with (CVT/SCT) and without (QC) Multidimensional Tunneling Contributions at 298 K

	$k(T)$ (1/s)			$k_H(T)/k_D(T)$	
	CM	QC	CVT/SCT	QC	CVT/SCT
theory	0.0087	1.77	132	5.9	18.3
expt[a]			275 ± 9[b]		17.2 ± 0.6,[b] 16.8 ± 0.5[c]

[a] 303 K. [b] Reference 50. [c] Reference 51.

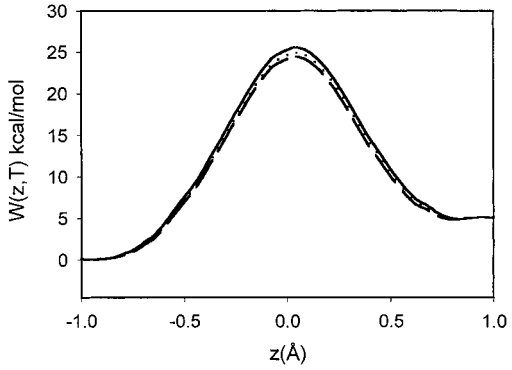

FIGURE 3. Classical mechanical PMF (solid curve) for hydride transfer and quasiclassical PMFs that include QM vibrational free energies for hydride- (dashed curve) and deuteride- (dotted curve) transfer reactions of xylose isomerase.

using static secondary zone transmission coefficients. The computed CM and QC potentials of mean force, the latter for both hydride and deuteride transfer, are shown in Figure 3. The two models yielded similar free energies of activation, in particular 25.0 kcal/mol classically and 23.7 kcal/mol including quantum mechanical vibrations. The figure shows that the QC ΔG_{act} is 24.1 kcal/mol for deuteride transfer, a difference of 0.4 kcal/mol from the hydride value.

Figure 4 depicts the variation in the average distance between the two Mg^{2+} ions as a function of the hydride-transfer reaction coordinate. The average Mg−Mg distance at the reactant state is in good accord with the second magnesium position found in the structure of the complex with D-glucose by Petsko and co-workers.[55] The simulations show that the magnesium distance increases by more than 1 Å during the hydride transfer. In the reactant state, the substrate 2 alkoxide anion is ligated to both magnesium ions, keeping them in close proximity; however, the product neutral carbonyl group produced by the

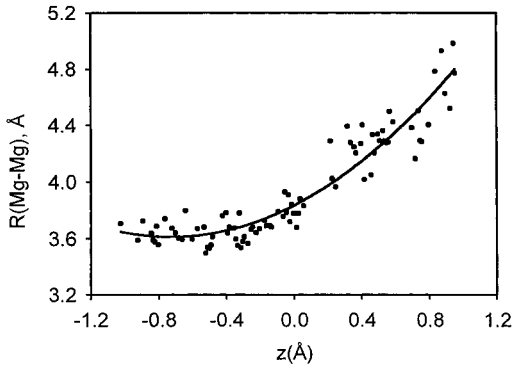

FIGURE 4. Computed Mg−Mg distance as a function of the hydride-transfer reaction coordinate for conversion of xylose to xylulose in xylose isomerase. The magnesium separation is accompanied by the migration of the hydride from C-2 to C-1, yielding a 1-alkoxide anion that favors strong binding with Mg-2.

hydride transfer provides a much weaker binding force. This leads to weaker interactions between the Mg ions and the O-2 oxygen, and the two Mg ions move to a greater separation.

Using the QC rate constants without tunneling, we obtain a KIE of 1.8 at 298 K. Our CVT/SCT calculations show that tunneling increases the rate constant by a factor of about 7 for the hydride transfer and increases the computed KIE to 3.8, which is in good accord with the experimental KIEs of 2.7−4.0 measured for enzymes from different species with glucose substrate and at 333 K.[58,59]

5. Conclusions

The examples presented above demonstrate the importance of quantum mechanical nuclear motion in reactions catalyzed by enzymes. In this Account, we have presented an overview of a combination of new procedures that provide a practical approach for including such effects in enzyme kinetics. Our approach features a combination of molecular dynamics simulations for determining the PMF that includes quantum vibrational free energies for enzyme reactions and VTST for dynamics calculations. Quantum effects are included in this procedure in three ways: (1) The electronic structure of the atoms in the catalytic center is treated quantum mechanically in order to calculate a realistic PES for the bond rearrangement process. (2) The discrete nature of quantum mechanical vibrational energies is incorporated in the treatment of nuclear motions. (3) Multidimensional tunneling contributions and dynamic recrossing transmission coefficients are included. The resulting method is called ensemble-

averaged VTST with multidimensional tunneling (EA-VTST/MT).

These procedures have been applied to proton abstractions catalyzed by enolase and methylamine dehydrogenase and hydride-transfer reactions catalyzed by liver alcohol dehydrogenase and xylose isomerase.[35−37,52,56] The effect on the free energy of activation of quantizing bound vibrations was found to be 2.1, 3.3, 1.8, and 1.3 kcal/mol for these reactions, respectively. Quantum mechanical tunneling further reduces the barrier heights by 0.3, 2.4, 0.8, and 1.1 kcal mol, respectively. Adding the two quantum effects gives a total lowering of ΔG_{act} that equals 2.4, 5.7, 2.6, and 2.4 kcal/mol due to (2) and (3) for these four reactions, in the order listed in this paragraph.

In all cases, we found that the computed KIEs are in agreement with experiment only when quantum mechanical tunneling contributions are included. In the case of liver alcohol dehydrogenase, coupled motions from the secondary hydrogen atom coupled to the reaction coordinate were found to be critical for interpreting the observed secondary KIEs. On the other hand, the largest quantum mechanical tunneling effects were found in the proton abstraction reaction by methylamine dehydrogenase, where tunneling increases the reaction rate by a factor of about 80.

Finally, we found that motions of the two magnesium ions in the active site of xylose isomerase are essential for mediating the proton- and hydride-transfer processes, and the ability of the present methods to incorporate quantum effects even in such a difficult case is attested by the fact that computed KIE for deuteride transfer in XyI is in good agreement with experiment when quantum mechanical tunneling contributions are included.

The limitations of the present methodology are that we need to start with an experimental crystal structure, the potential energy functions are not completely trustworthy although they are more accurate for the overall shape of the PES than methods based on a simple combination of empirical functions, and the dynamics is not treated in a fully coupled way when quantum effects are included. Nevertheless, we have had encouraging success in including the quantum effects, and we can look forward to applications to increasingly difficult problems in enzyme kinetics.

We thank the National Institutes of Health and the National Science Foundation for support of this work.

Note Added after ASAP Posting. On page 4 of this paper, left column, lines 3 and 4, "related to $\Delta G_{act}(T)$ by eq 3" was changed to "equal to $G^{GT}(T,z,\Omega)$". Line 6, ref 6 was changed to ref 5; line 24, ref 50 was changed to ref 37. The ASAP version of this paper that was posted on 4/15/2002 is correct.

References

(1) Truhlar, D. G.; Garrett, B. C. Variational transition-state theory. *Acc. Chem. Res.* **1980**, *13*, 440−448.

(2) Gao, J. Hybrid quantum mechanical/molecular mechanical simulations: an alternative avenue to solvent effects in organic chemistry. *Acc. Chem. Res.* **1996**, *29*, 298−305.

(3) Chuang, Y.-Y.; Cramer, C. J.; Truhlar, D. G. Interface of electronic structure and dynamics for reactions in solution. *Int. J. Quantum Chem.* **1998**, *70*, 887−896.

(4) Truhlar, D. G.; Isaacson, A. D.; Skodje, R. T.; Garrett, B. C. Incorporation of quantum effects in generalized-transition-state theory. *J. Phys. Chem.* **1982**, *86*, 2252−2261.

(5) Garcia-Viloca, M.; Alhambra, C.; Truhlar, D. G.; Gao, J. Inclusion of quantum-mechanical vibrational energy in reactive potentials of mean force. *J. Chem. Phys.* **2001**, *114*, 9953−9958.

(6) Truhlar, D. G.; Gordon, M. S. From force fields to dynamics: classical and quantal paths. *Science* **1990**, *249*, 491−498.

(7) Allison, T. C.; Truhlar, D. G. Testing the accuracy of practical semiclassical methods: Variational transition state theory with optimized multidimensional tunneling. In *Modern Methods for Multidimensional Dynamics Computations in Chemistry*; Thompson, D. L., Ed.; World Scientific: Singapore, 1998; pp 618−712.

(8) Pu, J.; Corchado, J. C.; Truhlar, D. G. Test of variational transition state theory with multidimensional tunneling contributions against an accurate full-dimensional rate constant calculation for a six-atom system. *J. Chem. Phys.* **2001**, *115*, 6266−6267.

(9) *Combined Quantum Mechanical and Molecular Mechanical Methods*; Gao, J., Thompson, M. A., Eds.; American Chemical Society: Washington, DC, 1998.

(10) Warshel, A.; Levitt, M. Theoretical studies of enzymic reactions. *J. Mol. Biol.* **1976**, *103*, 227−249.

(11) Singh, U. C.; Kollman, P. A. Combined ab initio quantum mechanical and molecular mechanical method for carrying out simulations. *J. Comput. Chem.* **1986**, *7*, 718−730.

(12) Field, M. J.; Bash, P. A.; Karplus, M. Combined quantum mechanical and molecular mechanical potential for molecular dynamics. *J. Comput. Chem.* **1990**, *11*, 700−733.

(13) Gao, J.; Xia, X. A priori evaluation of aqueous polarization effects through Monte Carlo QM-MM simulations. *Science* **1992**, *258*, 631−635.

(14) Thery, V.; Rinaldi, D.; Rivail, J. L.; Maigret, B.; Ferenczy, G. G. Quantum-mechanical computations on very large molecular systems—the local self-consistent-field method. *J. Comput. Chem.* **1994**, *15*, 269−282.

(15) Gao, J.; Amara, P.; Alhambra, C.; Field, M. J. Generalized hybrid orbital method for the treatment of boundary atoms in combined QM/MM calculations. *J. Phys. Chem. A* **1998**, *201*, 4714−4721.

(16) Dewar, M. J. S.; Zoebisch, E. G.; Healy, E. F.; Stewart, J. J. P. AM1: a new general purpose quantum mechanical molecular model. *J. Am. Chem. Soc.* **1985**, *107*, 3902−3909.

(17) Rossi, I.; Truhlar, D. G. Parameterization of NDDO wavefunctions using genetic algorithms. *Chem. Phys. Lett.* **1995**, *233*, 231−236.

(18) Mackerell, A. D., Jr.; Bashford,D.; Bellott, M.; Dunbrack, R. L., Jr.; Evanseck, J. D.; Field, M. J.; Fischer, S.; Gao, J.; Guo, H.; Ha, S.; Joseph-McCarthy, D.; Kuchnir, L.; Kuczera, K.; Lau, F. T. K.; Mattos, C.; Michnick, S.; Ngo, T.; Nguyen, D. T.; Prodhom, B.; Reiher, W. E., III; Roux, B.; Schlenkrich, M.; Smith, J. C.; Stote, R.; Straub, J.; Watanabe, M.; Wiórkiewicz-Kuczera, J.; Yin, D.; Karplus, M. All-atom empirical potential for molecular modeling and dynamics studies of proteins. *J. Phys. Chem. B* **1998**, *102*, 3586−3616.

(19) Jorgensen, W. L.; Chandrasekhar, J.; Madura, J. D.; Impey, R. W.; Klein, M. L. Comparison of simple potential functions for simulating liquid water. *J. Chem. Phys.* **1983**, *79*, 926−935.

(20) Truhlar, D. G.; Isaacson, A. D.; Garrett, B. C. Generalized transition state theory. In *Theory of Chemical Reaction Dynamics*; Baer, M., Ed.; CRC Press: Boca Raton, FL, 1985; Vol. 4, pp 65−137.

(21) Keck, J. C. Variational theory of reaction rates. *Adv. Chem. Phys.* **1967**, *13*, 85−121.

(22) Garrett; B. C.; Truhlar, D. G. Criterion of minimum state density in transition state theory. *J. Chem. Phys.* **1979**, *70*, 1593−1598.

(23) Liu, Y.-P.; Lu, D.-h.; Gonzalez-Lafont, A.; Truhlar, D. G.; Garrett, B. C. Direct dynamics calculation of the kinetic isotope effect for an organic hydrogen-transfer reaction, including corner-cutting tunneling in 21 dimensions. *J. Am. Chem. Soc.* **1993**, *115*, 7806−7817.

(24) Truhlar, D. G.; Kuppermann, A. Exact tunneling calculations. *J. Am. Chem. Soc.* **1971**, *93*, 1840−1851.

(25) Garrett, B. C.; Truhlar, D. G. Least-action variational method for calculating multidimensional tunneling probabilities. *J. Chem. Phys.* **1983**, *79*, 4931−4938.

(26) Marcus, R. A. Analytical mechanics of chemical reactions. *J. Chem. Phys.* **1966**, *45*, 4493−4499.

(27) Liu, Y.-P.; Lynch, G. C.; Truong, T. N.; Lu, D.-h.; Truhlar, D. G.; Garrett, B. C. Molecular modeling of the kinetic isotope effect for the [1,5]-sigmatropic rearrangement of *cis*-1,3-pentadiene. *J. Am. Chem. Soc.* **1993**, *115*, 2408−2415.

(28) Lim C.; Truhlar, D. G. Nonequilibrium effects in chemical kinetics. *J. Phys. Chem.* **1983**, *87*, 2683−2699.

(29) Karplus, M. Aspects of protein reaction dynamics. *J. Phys. Chem.* **2000**, *104*, 11−27.

(30) Hynes, J. T. Theory of reactions in solution. In *Theory of Chemical Reaction Dynamics*; Baer, M., Ed.; CRC: Boca Raton, FL, 1985; Vol. 4, pp 171−234.
(31) Chuang, Y.-Y.; Truhlar, D. G. Nonequilibrium solvation effects for a polyatomic reaction in solution. *J. Am. Chem. Soc.* **1999**, *121*, 10157−10167.
(32) Schenter, G. K.; Garrett, B. C.; Truhlar, D. G. Role of collective solvent coordinates and nonequilibrium solvation in charge-transfer reactions. *J. Phys. Chem. B* **2001**, *105*, 9672−9685.
(33) McQuarrie, D. A. *Statistical Mechanics*; Harper & Row: New York, 1973.
(34) Cramer, C. J.; Truhlar, D. G. Implicit solvation models. Equilibria, structure, spectra, and dynamics. *Chem. Rev.* **1999**, *99*, 2161−2200.
(35) Alhambra, C.; Gao, J.; Corchado, J. C.; Villà, J.; Truhlar, D. G. Quantum mechanical dynamical effects in an enzyme-catalyzed proton-transfer reaction. *J. Am. Chem. Soc.* **1999**, *121*, 2253−2258.
(36) Alhambra, C.; Corchado, J.; Sanchez, M. L.; Gao, J.; Truhlar, D. G. Quantum dynamics of hydride transfer in enzyme catalysis. *J. Am. Chem. Soc.* **2000**, *122*, 8197−8203.
(37) Alhambra, C.; Corchado, J.; Sanchez, M. L.; Garcia-Viloca, M.; Gao, J.; Truhlar, D. G. Canonical variational theory for enzyme kinetics with the protein mean force and multidimensional quantum mechanical tunneling dynamics. *J. Phys. Chem. B* **2001**, *105*, 11326−11340.
(38) Lauderdale, J. G.; Truhlar, D. G. Embedded-cluster model for the effect of phonons on hydrogen surface diffusion on copper. *J. Chem. Phys.* **1986**, *84*, 1843−1849.
(39) Kottalam, J.; Case, D. A. Dynamics of ligand escape from the heme pocket of myoglobin. *J. Am. Chem. Soc.* **1998**, *110*, 7690−7697.
(40) Bergsma, J. P.; Gertner, B. J.; Wilson, K. R.; Hynes, J. T. Molecular dynamics of a model S_N2 reaction in water. *J. Chem. Phys.* **1987**, *86*, 1356−1376.
(41) Neria, E.; Karplus, M. Molecular dynamics of an enzyme reaction: Proton transfer in TIM. *Chem. Phys. Lett.* **1997**, *267*, 23−30.
(42) Jorgensen, W. L.; Ravimohan, C. Monte Carlo simulation of differences in free energies of hydration. *J. Chem. Phys.* **1985**, *83*, 3050−3054.
(43) Brooks, C. L.; Brünger, A.; Karplus, M. Active-site dynamics in protein molecules: Stochastic boundary molecular-dynamics approach. *Biopolymers* **1985**, *24*, 843−865.
(44) Anderson, S. R.; Anderson, V. E.; Knowles, J. R. Primary and secondary kinetic isotope effects as probes of the mechanism of yeast enolase. *Biochemistry* **1994**, *33*, 10545−10555.
(45) Poyner, R. R.; Laughlin, L. T.; Sowa, G. A.; Reed, G. H. Toward identification of acid/base catalysts in the active site of enolase. *Biochemistry* **1996**, *35*, 1692−1699.
(46) Bahnson, B. J.; Park, D.-H.; Plapp, B. V.; Klinman, J. P. Unmasking of hydrogen tunneling in the horse LADH reaction by site-directed mutagenesis. *Biochemistry* **1993**, *32*, 5503−5507.
(47) Bahnson, B. J.; Klinman, J. P. Hydrogen tunneling in enzyme catalysis. *Methods Enzymol.* **1995**, *249*, 373−397.
(48) Billeter, S. R.; Webb, S. P.; Iordanov, T.; Agarwal, P. K.; Hammes-Schiffer, S. Hybrid approach for including electronic and nuclear quantum effects in molecular dynamics simulations of hydrogen transfer reactions in enzymes. *J. Am. Chem. Soc.* **2001**, *114*, 6925−6936.
(49) Villa, J.; Warshel, A. Energetics and dynamics of enzymatic reactions. *J. Phys. Chem. B* **2001**, *105*, 7887−7907.
(50) Brooks, H. B.; Jones, L. H.; Davidson, V. L. Deuterium kinetic isotope effect and stopped-flow kinetic studies of the quinoprotein MADH. *Biochemistry* **1993**, *32*, 2725−2729.
(51) Basran, J.; Sutcliffe, M. J.; Scrutton, N. S. Enzymic H-transfer requires vibration-driven extreme tunneling. *Biochemistry* **1999**, *38*, 3218−3222.
(52) Alhambra, C.; Sanchez, M. L.; Corchado, J.; Gao, J.; Truhlar, D. G. Quantum mechanical tunneling in MADH. *Chem. Phys. Lett.* **2001**, *347*, 512−518; erratum in press.
(53) Hu, H.; Liu, H.; Shi, Y. Reaction pathway of the isomerization of d-xylose catalyzed by the enzyme d-xylose isomerase. *Proteins* **1997**, *27*, 545−555.
(54) Nicoll, R. M.; Hindle, S. A.; MacKenzie, G.; Hillier, I. H.; Burton, N. A. Quantum mechanical/molecular mechanical methods and the study of kinetic isotope effects. *Theor. Chem. Acc.* **2001**, *106*, 105−112.
(55) Allen, K. N.; Lavie, A.; Petsko, G. A.; Ringe, D. Design, synthesis, and characterization of a potent xylose isomerase inhibitor, d-threonohydroxamic acid, and high-resolution X-ray crystallographic structure of the enzyme−inhibitor complex. *Biochemistry* **1995**, *34*, 3742−3749.
(56) Garcia-Viloca, M.; Truhlar, D. G.; Gao, J. To be published.
(57) Whitlow, M.; Howard, A. J.; Finzel, B. C.; Poulos, T. L.; Winborne, E.; Gilliland, G. L. Metal-mediated hydride shift mechanism for xylose isomerase based on the 1.6 A Streptomyces rubiginosus structures with xylitol and d-xylose. *Proteins* **1991**, *9*, 153−173.
(58) van Tilbeurgh, H.; et al. Protein engineering of xylose (glucose) isomerase from Actinoplanes missouriensis. 3. *Biochemistry* **1992**, *31*, 5467−5471.
(59) van Bastelaere, P. B. M.; Kersters-Hilderson, H. L. M.; Lambeir, A.-M. Wild-type and mutant d-xylose isomerase from Actinoplanes missouriensis. *Biochem. J.* **1995**, *307*, 135−142.

AR0100226